

## SOLAR NEUTRINO PHYSICS: SENSITIVITY TO LIGHT DARK MATTER PARTICLES

ILÍDIO LOPES<sup>1,2</sup> AND JOE SILK<sup>3,4,5</sup>(Dated: Received 2011 November 9; Accepted 2012 April 13)  
*Draft version February 26, 2022*

## ABSTRACT

Neutrinos are produced in several neutrino nuclear reactions of the proton–proton chain and carbon–nitrogen–oxygen cycle that take place at different radius of the Sun’s core. Hence, measurements of solar neutrino fluxes provide a precise determination of the local temperature. The accumulation of non-annihilating light dark matter particles (with masses between 5 GeV and 16 GeV) in the Sun produces a change in the local solar structure, namely, a decrease in the central temperature of a few percent. This variation depends on the properties of the dark matter particles, such as the mass of the particle and its spin-independent scattering cross-section on baryon-nuclei, specifically, the scattering with helium, oxygen, and nitrogen among other heavy elements. This temperature effect can be measured in almost all solar neutrino fluxes. In particular, by comparing the neutrino fluxes generated by stellar models with current observations, namely <sup>8</sup>B neutrino fluxes, we find that non-annihilating dark matter particles with a mass smaller than 10 GeV and a spin-independent scattering cross-section with heavy baryon-nuclei larger than  $3 \times 10^{-37} \text{ cm}^2$  produce a variation in the <sup>8</sup>B neutrino fluxes that would be in conflict with current measurements.

*Keywords:* dark matter– elementary particles – stars:evolution – stars:interiors – Sun:interior

## 1. INTRODUCTION

Dark matter makes up to 23% of all the known matter of the universe. This evidence comes from cosmological observations and numerical simulations (Komatsu et al. 2011), which suggest that most of the data can only be explained by the presence of a gravitational field caused by a new type of non-relativistic and non-baryonic fundamental particle (Munshi et al. 2011). If such particles exist, then they should be observed in direct detection experiments, and their effects should affect the internal structure of large self-gravitating bodies such as the Earth and our own Sun. Thus, it is no surprise that so much of the theoretical work and experimental efforts in the fields of astrophysics, cosmology and particle physics have been dedicated to the discovery of such fundamental particles, hitherto with little success.

Among the large number of dark matter particle candidates that have been proposed, Weakly Interacting Massive Particles (WIMPs) were until recently among the most popular. WIMPs arise in several extensions of the Standard Model of fundamental particles, such as the supersymmetric models of fundamental particles

(e.g., Jungman et al. 1996). In such classes of models, the lightest supersymmetric particle (LSP), the neutralino, or possibly the NLSP, is the most suitable candidate for dark matter. The neutralino is the natural WIMP candidate, a stable particle with a self-annihilation cross-section of the order of the weak-scale interaction. Unfortunately, this particle does not resolve the problem of baryon-anti-baryon asymmetry. Recently, several authors (e.g., Gudnason et al. 2006; Foadi et al. 2009; Hooper et al. 2005) have suggested a new fundamental particle that carries a conserved charge analogous to the baryon number and would resolve the aforementioned problem (Kaplan et al. 2009). This new type of matter, known as asymmetric dark matter and consisting mostly of Dirac particles, is particularly interesting since these candidates, like WIMPs, have interactions at the weak-scale and therefore sizeable scattering cross-sections with baryons, even if they do not annihilate (Kaplan et al. 2009). Asymmetric dark matter models (e.g., Farrar & Zaharijas 2006) suggest that such particles should have a mass of the order of a few GeV (e.g., Kang et al. 2011; Cohen et al. 2010).

In recent years, several underground experiments have been built to search for direct interactions of a dark matter particle with a baryon-nucleus (e.g., Bertone et al. 2005). Amongst current results, positive indication for dark matter was produced by the DAMA/LIBRA (Belli et al. 2011; Bernabei et al. 2008) and CoGeNT (Aalseth et al. 2011) experimental teams. Both of them have reported evidence of an annual modulation in the differential event rate, which they explain as a consequence of the motion of the Earth around the Sun (Drukier et al. 1986). The simplest interpretation of the data is to assign the observed annual modulation to be caused by the collision of a dark matter particle with a nucleus inside the detector. The dark matter particle is estimated to have a mass of the order of a few GeV (likely between 5 and 12 GeV), and a

<sup>1</sup> Centro Multidisciplinar de Astrofísica, Instituto Superior Técnico, Universidade Técnica de Lisboa, Av. Rovisco Pais, 1049-001 Lisboa, Portugal; ilidio.lobes@ist.utl.pt, ilopes@uevora.pt

<sup>2</sup> Departamento de Física, Escola de Ciência e Tecnologia, Universidade de Évora, Colégio Luis António Verney, 7002-554 Évora - Portugal

<sup>3</sup> Institut d’Astrophysique de Paris, UMR 7095 CNRS, Université Pierre et Marie Curie, 98 bis Boulevard Arago, Paris 75014, France; silk@astro.ox.ac.uk

<sup>4</sup> Department of Physics and Astronomy, 3701 San Martin Drive, The Johns Hopkins University, Baltimore MD 21218, USA

<sup>5</sup> Beecroft Institute of Particle Astrophysics and Cosmology, 1 Keble Road, University of Oxford, Oxford OX1 3RH UK

spin-independent scattering cross-section off baryons on the order of  $10^{-40} \text{ cm}^2$ . Both experiments show identical positive detections, yet the DAMA experiment is favorable to a larger scattering cross-section than the CoGeNT experiment. Unfortunately, other direct dark matter search experiments, XENON10/100 (Angle et al. 2011; Aprile et al. 2011) and CDMS (Ahmed et al. 2011) found null detections, therefore these experimental results are in disagreement with the previous ones. Most recently, CRESST has also reported unexplained events in a similar mass range (Brown et al. 2012).

There is an equally serious objection from both cosmic microwave background and dwarf galaxy studies. WMAP7 uses acoustic peak damping to constrain any annihilation contribution to early ionization (Cirelli et al. 2012), FERMI stacking of dwarf galaxies shows similar limits on the annihilation cross-section as a function of the mass (Geringer-Sameth & Koushiappas 2011). In the case of thermal relic cross-sections, dark matter particles with masses below 10-30 GeV are excluded. Nevertheless, several authors (e.g., Chang et al. 2010; Farina et al. 2011; Hooper & Kelso 2011; Del Nobile et al. 2011) have proposed various theoretical solutions to overcome the apparent inconsistencies in the data interpretation. Such theoretical proposals reconcile all the experimental results: DAMA/LIBRA and CoGeNT experiments are no longer excluded by the CDMS and XENON experiments; and the DAMA/LIBRA and CoGeNT experimental positive detections, previously, leading to distinct and unrelated scattering cross-sections, now have the same values. Likewise, the annihilation constraint is weakened if some fraction of the WIMPs do not annihilate, or if the relic cross-section decouples from the current epoch cross-section by allowing for s-wave suppression of the relic cross-section (Imminiyaz et al. 2011).

One of the more appealing suggestions is the possibility of the dark matter particle being coupled unequally to the nucleons (protons and neutrons) of the colliding nuclei because of isospin violation. Usually, the dark matter particle is considered to couple equally with protons and neutrons. Accordingly, the independent scattering cross-section of heavy elements scales with  $A^2$ , where  $A$  is the atomic number of the nucleus. If the dark matter particles couple differently to protons and neutrons, these lead to a quite distinct interpretation of direct dark matter searches. This nuclear mechanism is known as isospin coupling violation (e.g., Kurylov & Kamionkowski 2004; Giuliani 2005; Cotta et al. 2009). It was shown that a change of the strength of coupling of the dark matter particle with protons and neutron allows the reconciliation of all of the current experiments (Chang et al. 2010; Farina et al. 2011; Hooper & Kelso 2011; Del Nobile et al. 2011). In such cases, the proton scattering cross-section for the independent interaction increases by  $10^2$ – $10^3$  relative to the usual results, leading to an effective independent scattering cross-section with values between  $10^{-40} \text{ cm}^2$  and  $10^{-36} \text{ cm}^2$  (Del Nobile et al. 2011; Aalseth et al. 2011; Hooper & Kelso 2011). We point out here that these types of dark matter particles can modify the structure of a star like the Sun, leading to a quite different flux of solar neutrinos.

The measurement of the solar neutrino fluxes offers a

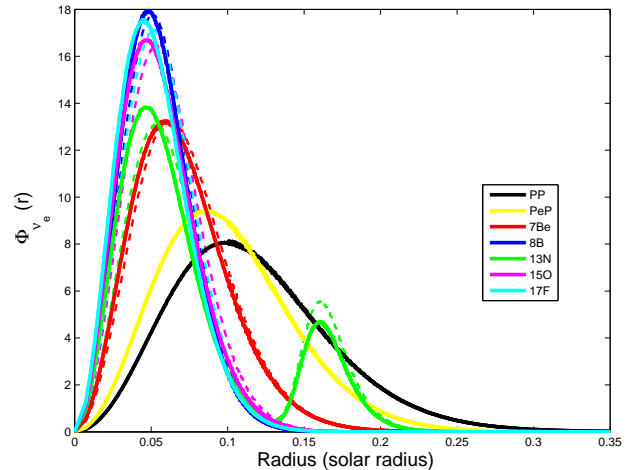


**Figure 1.** The electron-neutrino flux produced in the various nuclear reactions of the PP chains and CNO cycle for two distinct solar models. (i) continuous curves: the solar model is in agreement with the most current helioseismology diagnostic, and other solar standard models published in the literature Bahcall et al. (2005); Guzik & Mussack (2010). (ii) dotted curves: a solar model evolved in a halo of dark matter particles with mass of 7 GeV and independent scattering cross-section  $\sigma_{SI} = 10^{-36} \text{ cm}^2$  (other parameters see text). The neutrino flux produced in the various nuclear reactions is computed for a revised version of the solar model and the most updated microscopic physics data.

distinct method for a diagnostic of the central regions of the Sun. In past decades, the main goal of solar neutrino detection was to study the particle properties of the neutrinos themselves. Now that neutrino oscillations are well-established, detectors are arriving at a stage where information on the solar core can be extracted from precise measurements of the solar neutrino spectrum. This enables a search for dark matter in the core of the Sun.

In the next section, we review the main physical processes related with the capture of dark matter by a star like the Sun. In Section 3, we present a detailed discussion about the production of neutrinos in the solar core and explain the impact of dark matter on the production of neutrino fluxes. In the final section we discuss the results obtained relative to the current experimental bounds.

## 2. SUN'S EVOLUTION IN A NON-ANNIHILATING DARK MATTER PARTICLE HALO

The formation and evolution of the Sun inside a dark matter halo is similar to a normal star of population II, although there are some important modifications (Scott, P. C. et al. 2008; Casanellas & Lopes 2009; Scott et al. 2009; Lopes et al. 2011). The Sun by means of its large gravitational field captures an important amount of dark matter particles during its evolution (Cumberbatch et al. 2010; Taoso et al. 2010). The accumulation of dark matter inside the star leads to the formation of a dark matter core. The effect on the structure of the star is primarily to provide an additional mechanism for the transfer of energy, which in some cases significantly reduces the temperature gradient, thereby causing the stellar core to become almost isothermal (Lopes & Silk 2002, 2010b). In some dark matter scenarios, dark matter annihilation provides the star with an extra source of energy which changes the evolution path of the star (Casanellas & Lopes 2011a,b). Nevertheless, such physical processes are not relevant for

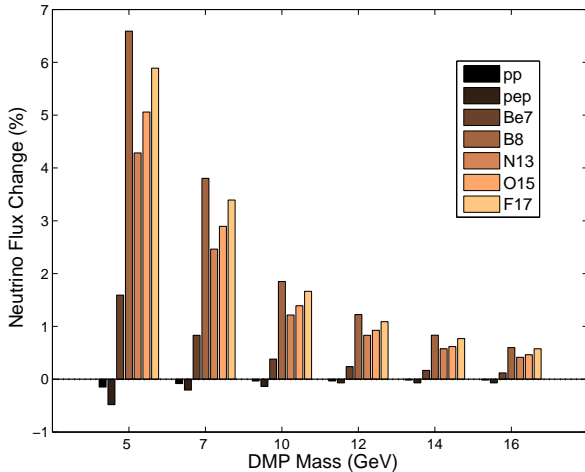


**Figure 2.** Percentage decrease changes in the solar neutrino flux,  $(\Phi_{ssm} - \Phi_{DM})/\Phi_{ssm}$ .  $\Phi_{DM}$  is one of the neutrino fluxes for the PP chain ( $pp$ ,  $pep$ ,  ${}^7\text{Be}$  and  ${}^8\text{B}$ ) or the CNO cycle ( ${}^{13}\text{N}$ ,  ${}^{15}\text{O}$  and  ${}^{17}\text{F}$ ) in the case of non-annihilating dark matter particles accumulate in the center of the Sun. The dark matter particles scatter with nucleons with  $\sigma_{SD} = 10^{-40} \text{ cm}^2$  and  $\sigma_{SI} = 10^{-36} \text{ cm}^2$ . The mass of the dark matter particle is indicated in the figure. The neutrino flux percentage change of each species is compared to the current flux values as predicted by our solar standard model.

the dark matter models discussed here.

The efficiency of the energy transport provided by dark matter particles depends on the average distance traveled by particles between consecutive collisions, i.e., the mean free path of the dark matter particle. If the mean free path is short compared with the dark matter scale height, then the energy transfer proceeds by conduction. Alternatively, if the mean free path is large, the successive collisions are widely separated, so that the energy transfer proceeds within the Knudsen regime (Lopes & Silk 2002). In most of the dark matter scenarios discussed in this paper, the energy transport is dominated by conduction, although, the code has an implementation of the transport of energy by dark matter in both regimes (Lopes et al. 2002, 2011).

The amount of dark matter captured by the star, among other parameters, depends on the mass of the dark matter particles  $m_\chi$  and the collision cross-section of dark matter particles with baryons (Gould 1987). Two leading parameters define the scattering of the dark matter particles with the baryon nuclei: the spin-dependent scattering cross-section  $\sigma_{SD}$  that is only relevant for hydrogen nuclei; and the spin-independent scattering cross-section  $\sigma_{SI}$  that defines the interaction of the dark matter particles with the heavy nuclei. The values of  $\sigma_{SI}$  used in the calculation include the values found by the new interpretation of experimental results, comprised by the DAMA/LIBRA and CoGeNT data. If the value of  $\sigma_{SI}$  is larger or equal to  $\sigma_{SD}$ , the capture of dark matter particles is dominated by the collisions with heavy nuclei, rather than by collisions with hydrogen (Lopes et al. 2011).

The capture rate is computed numerically from the integral expression of Gould (1987) implemented as indicated in Gondolo et al. (2004). If not stated otherwise, we assume that the density of dark matter in the halo is  $0.3 \text{ GeV cm}^{-3}$ , the stellar velocity of the Sun is  $220 \text{ kms}^{-1}$  and the Maxwellian velocity dispersion is  $270 \text{ kms}^{-1}$ .

The stellar code explicitly follows the capture rate of the dark matter particles by the different chemical elements present inside the Sun, some of them changing in isotopic abundance during the Sun’s evolution. The paper (Lopes et al. 2011) presents a detailed discussion about the properties of dark matter particles, as well as the impact that the uncertainties of the dark matter parameters have on the evolution of the Sun and stars.

Our evolution code is a modified version of the one-dimensional stellar evolution CESAM (Morel 1997). The code has up-to-date and very refined microscopic physics (updated equation of state, opacities, nuclear reactions rates, and an accurate treatment of microscopic diffusion of heavy elements), including the solar mixture of Asplund et al. (2005). The solar models are calibrated to the present solar radius  $R_\odot = 6.9599 \times 10^{10} \text{ cm}$ , luminosity  $L_\odot = 3.846 \times 10^{33} \text{ erg s}^{-1}$ , mass  $M_\odot = 1.989 \times 10^{33} \text{ g}$ , and age  $t_\odot = 4.54 \pm 0.04 \text{ Gyr}$  (e.g., Turck-Chieze & Couvidat 2011). The models are required to have a fixed value of the photospheric ratio  $(Z/X)_\odot$ , where  $X$  and  $Z$  are the mass fraction of hydrogen and the mass fraction of elements heavier than helium. The value of  $(Z/X)_\odot$  is determined according to the solar mixture proposed by Asplund et al. (2005). Our reference model is a solar standard model (Turck-Chieze & Lopes 1993) that shows acoustic seismic diagnostics and solar neutrino fluxes identical to other solar standard models (Guzik & Mussack 2010; Serenelli et al. 2009; Bahcall et al. 2005; Turck-Chieze et al. 2010).

We have computed the evolution of the Sun in several dark matter particle scenarios, where  $m_\chi$  takes values between 5 and 16 GeV, and the spin-independent scattering cross-section  $\sigma_{SD}$  takes values between  $10^{-41}$  and  $10^{-34} \text{ cm}^2$ . The spin-dependent scattering cross-section  $\sigma_{SD}$  is approximately  $10^{-40} \text{ cm}^2$ . This choice of parameters covers the parameter range of the experimental results of the direct dark matter searches discussed in the previous section.

The Sun evolves from the beginning of the pre-main sequence until its present age. Each solar model has more than 2000 layers, and it takes more than 80 time steps to arrive at the present age. In the scenarios where a large amount of dark matter is captured, a single solar model can have more than 140 time steps before arriving at the present Sun. At each epoch, the structure equations are solved with an accuracy of  $10^{-5}$ . For each set of dark matter parameters, a solar-calibrated model is obtained by automatically adjusting the helium abundance and the convection mixing length parameter until the total luminosity and the solar radius are within  $10^{-5}$  of the present solar values. Typically, a calibrated solar model is obtained after a sequence of 10 intermediate solar models, although the models with a large concentration of dark matter need more than 20 intermediate models. In the next section, we discuss the impact of such models on the production of solar neutrino fluxes.

### 3. SOLAR NEUTRINOS AND DARK MATTER

Neutrinos are generated in the interior of the Sun as a by-product of the fusion processes that power the solar energy production, mainly by the proton-proton (PP) fusion chain (98%), and with a small contribution from the catalytic carbon–nitrogen–oxygen (CNO)

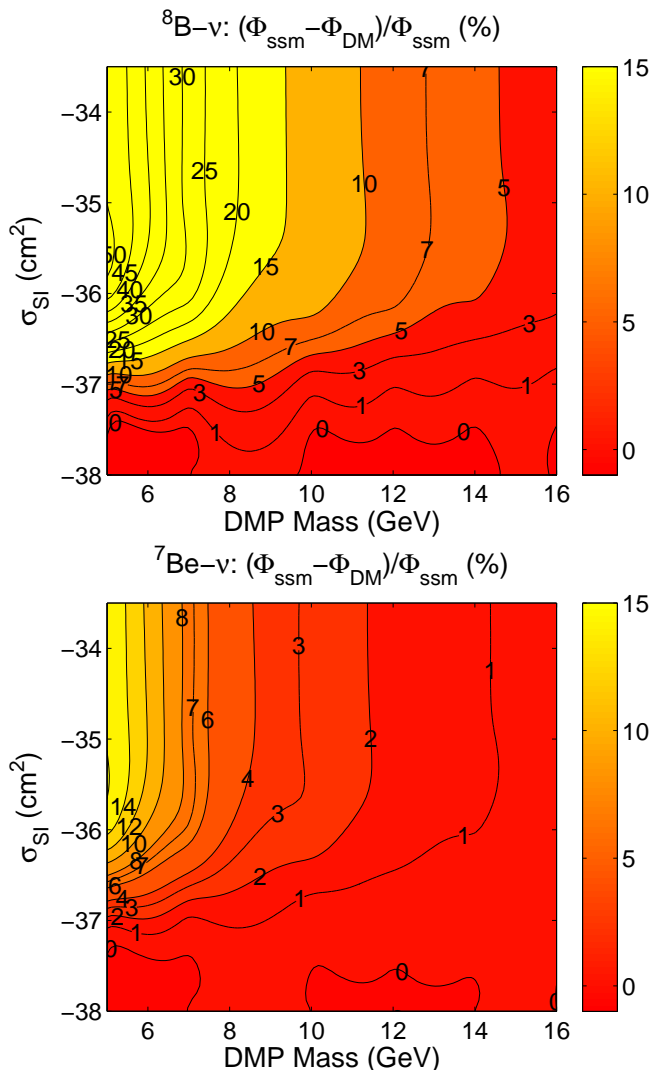


**Figure 3.** Percentage decrease changes in the solar neutrino flux of  $\Phi_\nu(^8\text{B})$  and  $\Phi_\nu(^7\text{Be})$  computed as  $(\Phi_{ssm} - \Phi_{DM})/\Phi_{ssm}$ .  $\Phi_{DM}$  is one of the following fluxes  $\Phi_\nu(^8\text{B})$  (top figure) and  $\Phi_\nu(^7\text{Be})$  (bottom figure). Iso-curves for neutrino fluxes in the plane of the dark matter particle independent scattering cross-section ( $\sigma_{SI}$ ) vs. the dark matter particle mass ( $m_\chi$ ). The other parameters of the dark matter particles and the stellar physics can be found in the main text. The neutrino fluxes of the solar standard model are used as reference. Both panels use the same contour colour scheme.

cycle (2%). Accordingly to the modern theory of neutrino oscillations (Hernandez 2010), solar neutrinos fluctuate between three possible flavors during their travel throughout space. Although solar neutrinos are generated in the Sun’s core with electron flavor, depending on their energy, a significant part of them are converted into another flavor. The conversion from electron flavor is accomplished by means of two possible mechanisms: the neutrino vacuum oscillations and the Mikheyev–Smirnov–Wolfenstein (MSW) neutrino oscillations or matter neutrino oscillations (Gonzalez-Garcia & Maltoni 2008; Fogli et al. 2011; Apollonio & Baldini 1999).

The change of structure of the solar core, caused by the presence of dark matter, leads to variations of the temperature and density profiles, which in turn produce a visible variation in the production of neutrino fluxes (Taoso et al. 2010; Frandsen & Sarkar 2010;

Cumberbatch et al. 2010). This variation in the neutrino fluxes is mainly caused by a change in the rate of the production of neutrinos, due to the decrease of the local temperature. This process is accompanied by a small increase of the density profile, for which the impact on the MSW neutrino oscillation mechanism is negligible. For this reason, we will restrict our analysis to the total neutrino flux production and neglect the contribution to neutrino oscillations.

In the Sun’s core, the neutrino emission regions occur in a sequence of shells, following closely the location of nuclear reactions, orderly arranged in a sequence of decreasing temperatures, from the center towards the surface. In the case of our solar standard model, the maximum neutrino emission of the PP nuclear reactions,  $pp$ ,  $pep$ ,  $^7\text{Be}$  and  $^8\text{B}$ , occurs at 10%, 8%, 6% and 4% of the solar radius. Figure 1 shows the location of the different neutrino emission regions for several nuclear reactions.

The presence of dark matter particles inside the star produces significant modifications of the solar neutrino fluxes (see Figure 2), caused by the reduction of the temperature and by changes in the neutrino emission regions (see Figure 1). The  $pp$  and  $pep$  nuclear reactions have neutrino emission regions that extend from the center up to 30% and 25% of the solar radius. Both nuclear reactions are strongly dependent on the total luminosity of the star. As a consequence, different calibrated solar models (with or without dark matter) maintain the same neutrino emission shells. In Figure 1, the  $pp$  and  $pep$  emission shells are identical for both solar models. Instead, the  $^8\text{B}$  and  $^7\text{Be}$  neutrino emission shells with a width of 15% and 22% of the solar radius have slightly changed the location of their maxima. This effect has a strong impact on the neutrino fluxes from these nuclear reactions (see Figure 2), since the  $\Phi_\nu(^8\text{B})$  neutrino flux dependence on the central temperature  $T_c$  is proportional to  $T_c^{24}$  and  $\Phi_\nu(^7\text{Be})$  is proportional to  $T_c^{10}$  (Turck-Chieze & Lopes 1993; Bahcall & Ulmer 1996; Bahcall 2002). Likewise, the  $\Phi_\nu(pep)$  is proportional to  $T_c^{-2.4}$  (Bahcall & Ulmer 1996). It follows that  $\Phi_\nu(^8\text{B})$  is a more sensitive probe of the central temperature than  $\Phi_\nu(^7\text{Be})$ .

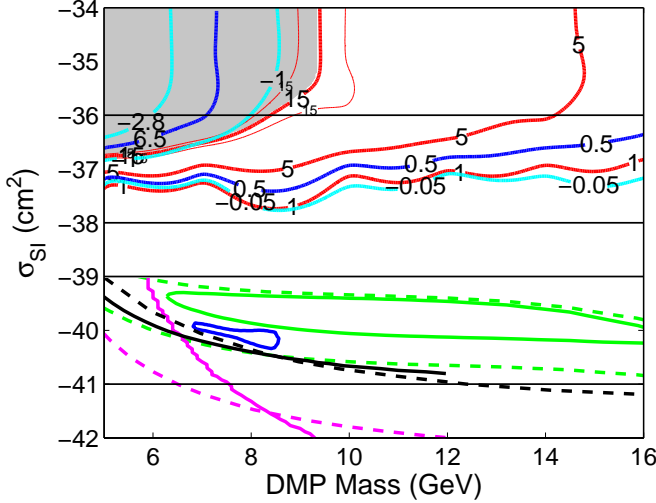
The neutrino emission shell of the CNO cycle nuclear reactions,  $^{15}\text{O}$ ,  $^{17}\text{F}$  and  $^{13}\text{N}$  has a behavior identical to that of the  $^8\text{B}$  neutrino emission shell. The only exception is the  $^{13}\text{N}$  nuclear reaction that has a second emission shell located between 12% and 25% of the Sun’s radius, with a maximum emission at 16% of the solar radius. The neutrino fluxes due to such nuclear reactions, similar to  $^8\text{B}$ , are very sensitive to the presence of dark matter in the Sun’s core.

Figure 2 shows the change of neutrino fluxes relative to the solar standard model for several dark matter scenarios of light dark matter particles. The neutrinos produced in the central regions are more affected than the ones produced in the more external layers. Furthermore, the dark matter particles with smaller masses produce a more extended dark matter core leading to a larger effect on the production of neutrino fluxes.

#### 4. DISCUSSION AND CONCLUSION

The  $\Phi_\nu(^8\text{B})$  and  $\Phi_\nu(^7\text{Be})$  neutrino fluxes are presented as a variation relative to the values of the neutrino fluxes





**Figure 4.** Exclusion Plot  $m_\chi - \sigma_{SI}$  for current dark matter searches and future neutrino experiments : (i) – Current experimental allowed regions and exclusion contours: CoGeNT Annual Modulation ROI (Aalseth et al. 2011) (closed blue curve), and DAMA/LIBRA assuming no ion channeling (Savage et al. 2009; Bernabei et al. 2008) with a  $3\sigma$  CL (solid green curve) and  $5\sigma$  CL (dashed green curve); the XENON 10 (90%CL) (Angle et al. 2011) (dashed magenta curve) and XENON100 (Aprile et al. 2011) (solid magenta curve) exclusion contours; the CDMS II limit (Ahmed et al. 2011) (solid black curve); the SIMPLE limit (Felizardo et al. 2012) (dashed black curve). (ii) – iso-contour of solar neutrino fluxes expected percentage variations  $((\Phi_{ssm} - \Phi_{DM})/\Phi_{ssm})$  for dark matter solar models.  $\Phi_{DM}$  is one of the following fluxes:  $\Phi_\nu(^8B)$  - solid red curve 15%, 5%, 1%,  $\Phi_\nu(^7Be)$  - solid blue curve 6.5%, 0.5% and  $\Phi_\nu(pep)$  - solid cyan curve -2.8%, -1.0%, -0.05%. (iii) – The gray region corresponds to values of  $\Phi_\nu(^8B)$  neutrino flux larger than 15% (red curve), the two 15%-thin-red lines correspond to assuming an experimental error of 2% on the measurement of  $\Phi_\nu(^8B)$  (LENA experiment targets a 1% error bar). (iv) – The region between the continuous black straight-lines corresponds to the location of the theoretical dark matter candidates: experimental data is contradictory when dark matter interaction is interpreted assuming the conservation of iso-spin ( $\sigma_{SI}$  with values  $10^{-41} - 10^{-39} \text{cm}^2$ ), and all the dark experimental data is reconciled when dark matter interaction is interpreted assuming iso-spin violation, inelastic scattering or some other similar theoretical mechanism ( $\sigma_{SI}$  with values  $10^{-38} - 10^{-36} \text{cm}^2$ ).

in the Solar Standard Model. This procedure facilitates the comparison of these results with the data from the Sudbury Neutrino Observatory (SNO) and Borexino detectors.

The current neutrino experiments suggests that the expected value for the  $^8B$  neutrino flux in the case of no neutrino oscillations (or electron neutrinos; including the theoretical uncertainty on the  $^8B$  flux in the solar standard model) is  $\Phi_\nu(^8B) = 5.05^{+0.19}_{-0.20} \times 10^6 \text{cm}^2 \text{s}^{-1}$  for the SNO experiment (Aharmim et al. 2010), and  $\Phi_\nu(^8B) = 5.88 \pm 0.65 \times 10^6 \text{cm}^2 \text{s}^{-1}$  for the Borexino experiment (Bellini et al. 2010). Furthermore, the Borexino experiment measures  $^7Be$  solar neutrino rates with an accuracy better than 5%. This corresponds to a  $^7Be$  neutrino flux  $\Phi_\nu(^7Be) = 4.87 \pm 0.24 \times 10^9 \text{cm}^2 \text{s}^{-1}$ , under the assumption of the MSW-LMA scenario of solar neutrino oscillations (Bellini et al. 2011; Arpesella et al. 2008). These values are in agreement with the neutrino predictions of the current solar standard model (Turck-Chieze et al. 2010; Serenelli et al. 2011). Nevertheless, the Sun's core seems to be slightly hotter than

expected, since the  $\Phi(^8B)$  value measured by Borexino and SNO is higher than the value predicted by the current solar standard model. This discrepancy is larger in the case of Borexino than for the SNO measurement. Furthermore, this result is validated by the Borexino measurement of  $\Phi_\nu(^7Be)$  which is sensitive to a region slightly off the Sun's center (see Figure 1).

Recently, the Borexino experiment made the first measurement of the *pep* neutrinos,  $\Phi_\nu(pep) = 1.6 \pm 0.3 \times 10^8 \text{cm}^2 \text{s}^{-1}$  (Bellini et al. 2012). This preliminary measurement of  $\Phi_\nu(pep)$  also indicates that the Sun is hotter than the solar standard model. This diagnostic is very interesting because  $\Phi_\nu(pep)$  is strongly dependent on the luminosity of the star. Therefore, it is an indirect measurement of the total energy (luminosity) produced in the nuclear region, without the complications related with the transport of energy by radiation and convection of the more external layers of the star. Once the accuracy is improved in such measurements, this will be a powerful test to the nuclear region of solar models.

Dark matter particles with masses smaller than 5 GeV are not considered because evaporation becomes important and a large number of dark matter particles then escape the gravitational field of the star, significantly reducing the impact on the Sun's core (Gould 1990). Dark matter particles with masses above 12 GeV produce a very small dark matter core and their effect in the Sun's structure diminishes rapidly, leading to variations of at most a few percent on the predicted neutrino fluxes (Spergel & Press 1985). Moreover, for the light dark matter particles with masses between 5 and 12 GeV, the size of the affected core region is comparable to that of the neutrino generation region, thus reducing the neutrino count expected to be measured in the terrestrial neutrino detectors.

Figure 3 shows a systematic study of the dark matter parameter space by varying the mass  $m_\chi$  and the spin-independent scattering cross-section  $\sigma_{SI}$  of the dark matter particles. A set of more than a hundred solar models was computed for different dark matter parameters. These results are qualitatively consistent with previous results in the case of the spin-dependent scattering cross-section (Lopes & Silk 2010a,b). In the  $m_\chi$  vs.  $\sigma_{SI}$  plane, the iso-contours corresponding to  $\Phi_\nu(^8B)$  and  $\Phi_\nu(^7Be)$  show variations up to 50% and 30% relatively to the solar standard model. The  $\Phi_\nu(^8B)$  variation is larger than  $\Phi_\nu(^7Be)$ , because  $^8B$  neutrinos are produced in a more central region than  $^7Be$  neutrinos, and therefore have a larger sensitivity (see Figure 2).

The current modeling of the microscopic physics (nuclear reactions rates, microscopic diffusion, radiative transfer and elemental abundances) in the Sun presents some significant uncertainties in the neutrino fluxes and acoustic mode predictions. Nevertheless, several authors (Bahcall et al. 2005; Turck-Chieze et al. 2010; Guzik & Mussack 2010) have shown that the largest contribution to the theoretical uncertainties comes from new measurements of the surface elemental abundances (Asplund et al. 2009; Serenelli et al. 2009). Indeed, the scientific community agrees that the new abundance determinations are the most reliable. If we consider the combined experimental and theoretical uncertainties of  $\Phi_\nu(^8B)$  to be of the order of 15%, i.e.

$\Delta\Phi_\nu(^8\text{B})/\Phi_\nu(^8\text{B}) \sim 15\%$ , then the dark matter particles for which the variation of  $\Phi_\nu(^8\text{B})$  is larger than 15% can be excluded. This corresponds approximately to rejecting dark matter particle candidates with low mass and large scattering cross-sections, i.e.,  $m_\chi \leq 11$  GeV and  $\sigma_{\text{SD}} \geq 3 \times 10^{-37} \text{ cm}^2$ . Moreover, the  $^8\text{B}$  flux variation is equivalent to a variation of the central temperature,  $\Delta T_c/T_c$  to be of 0.6%. Assuming that the other neutrino flux sources are affected by the same uncertainty, the dark matter candidates excluded have  $^7\text{Be}$  and  $pep$  neutrino fluxes, such as  $\Delta\Phi_\nu(^7\text{Be})/\Phi_\nu(^7\text{Be}) \geq 6.25\%$  or  $\Delta\Phi_\nu(pep)/\Phi_\nu(pep) \leq -1.5\%$ .

Figure 4 shows the allowed regions and exclusion contours of current dark matter searches and the solar neutrino flux variations of several dark matter-modified solar models. The current positive detections of dark matter experiments such as DAMA/LIBRA and CoGeNT occur for values of  $\sigma_{\text{SI}}$  that do not affect the evolution of the Sun,  $10^{-41} \text{ cm}^2 \leq \sigma_{\text{SI}} \leq 3 \times 10^{-39} \text{ cm}^2$ . This situation has changed with a new interpretation of the experimental data results, which evokes the possibility that if dark matter interactions with ordinary matter do not conserve iso-spin, as several authors have showed, then all the direct detection experimental data can be reconciled (e.g., Farina et al. 2011). Other processes such as inelastic scatterings and channeling, velocity-dependent form factors and momentum-dependent form factors are among the various processes that may significantly increase the value of the spin-independent scattering cross-section of the dark matter particles (e.g., Farina et al. 2011). Such new models suggest that the dark matter particle candidates have  $\sigma_{\text{SI}}$  values within reach of the solar neutrino experiments,  $10^{-38} \text{ cm}^2 \leq \sigma_{\text{SI}} \leq 3 \times 10^{-36} \text{ cm}^2$ .

In the near future with the improvement of the sensitivity of the detectors, it will be possible to reduce the uncertainties in the  $\Phi_\nu(^8\text{B})$ ,  $\Phi_\nu(^7\text{Be})$  and  $\Phi_\nu(pep)$ , as well as to measure the neutrino fluxes produced in the CNO cycle.

The CNO neutrino fluxes can provide an additional test of the accretion of dark matter in the Sun's core, once the  $\Phi_\nu(^{13}\text{N})$ ,  $\Phi_\nu(^{15}\text{O})$  and  $\Phi_\nu(^{17}\text{F})$  electronic neutrino fluxes have a dependence on  $T_c$  of 24.4, 27.1 and 27.8, identical to or larger than the neutrino fluxes of  $^8\text{B}$  (Bahcall & Ulmer 1996). The high-statistics data expected to be collected by the upgraded versions of present neutrino detectors, such as the SNO and Borexino, or even more so by the new neutrino detector Low Energy Neutrino Astrophysics (LENA), would allow a precise determination of such solar neutrino fluxes. It is expected that LENA will allow measurement of  $^8\text{B}$  neutrinos with a precision of 1% (Wurm et al. 2011). As illustrated in Figure 4, if an error bar of 2% in the measurement of  $\Phi_\nu(^8\text{B})$  is obtained at the experimental level, this will allow us to infer an even more significant constraint on the parameters of possible dark matter particles.

Such detailed determinations of neutrino fluxes by future neutrino experiments will provide the means to precisely probe the central Sun's core temperature, and by doing so, the contents of dark matter. In particular, this will allow a better screening of dark matter particle candidates such as those postulated to fit the data of the DAMA/LIBRA and CoGeNT experiments.

This work was supported in part by grants from "Fundação para a Ciência e Tecnologia" (SFRH/BD/44321/2008), "Fundação Calouste Gulbenkian", and the NSF (grant OIA-1124453). We thank the anonymous referee for the useful comments and suggestions that improved the quality of the paper.

## REFERENCES

- Aalseth C. E. et al., 2011, *Physical Review Letters*, 107, 141301  
 Aharmim B. et al., 2010, *Physical Review C*, 81, 55504  
 Ahmed Z. et al., 2011, *Physical Review Letters*, 106, 131302  
 Angle J. et al., 2011, *Physical Review Letters*, 107, 51301  
 Apollonio M., Baldini A., 1999, *Physics Letters B*, 466, 415  
 Aprile E. et al., 2011, *Physical Review Letters*, 107, 131302  
 Arpesella C. et al., 2008, *Physics Letters B*, 658, 101  
 Asplund M., Grevesse N., Sauval A. J., 2005, *Magnetic Fields Across the Hertzsprung-Russell Diagram*, 336, 25  
 Asplund M., Grevesse N., Sauval A. J., Scott P., 2009, *Annual Review of Astronomy and Astrophysics*, 47, 481  
 Bahcall J. N., 2002, *Physical Review C*, 65, 25801  
 Bahcall J. N., Serenelli A. M., Basu S., 2005, *The Astrophysical Journal*, 621, L85  
 Bahcall J. N., Ulmer A., 1996, *Physical Review D (Particles)*, 53, 4202  
 Belli P., Bernabei R., Bottino A., Cappella F., Cerulli R., Fornengo N., Scopel S., 2011, *Physical Review D*, 84, 55014  
 Bellini G. et al., 2012, *Physical Review Letters*, 108, 51302  
 Bellini G. et al., 2011, *Physical Review Letters*, 107, 141302  
 Bellini G. et al., 2010, *Physical Review D*, 82, 33006  
 Bernabei R. et al., 2008, *The European Physical Journal C*, 56, 333  
 Bertone G., Hooper D., Silk J., 2005, *Physics Reports*, 405, 279  
 Brown A., Henry S., Kraus H., McCabe C., 2012, *Physical Review D*, 85, 21301  
 Casanellas J., Lopes I., 2009, *The Astrophysical Journal*, 705, 135  
 Casanellas J., Lopes I., 2011a, *The Astrophysical Journal Letters*, 733, L51  
 Casanellas J., Lopes I., 2011b, *Monthly Notices of the Royal Astronomical Society*, 410, 535  
 Chang S., Liu J., Pierce A., Weiner N., Yavin I., 2010, *Journal of Cosmology and Astroparticle Physics*, 08, 018  
 Cirelli M., Panci P., Servant G., Zaharijas G., 2012, *Journal of Cosmology and Astroparticle Physics*, 03, 015  
 Cohen T., Phalen D. J., Pierce A., Zurek K. M., 2010, *Physical Review D*, 82, 56001  
 Cotta R. C., Gainer J. S., Hewett J. L., Rizzo T. G., 2009, *New Journal of Physics*, 11, 5026  
 Cumberbatch D. T., Guzik J. A., Silk J., Watson L. S., West S. M., 2010, *Physical Review D*, 82, 103503  
 Del Nobile E., Kouvaris C., Sannino F., 2011, *Physical Review D*, 84, 27301  
 Drukier A. K., Freese K., Spergel D. N., 1986, *Physical Review D (Particles and Fields)*, 33, 3495  
 Farina M., Pappadopulo D., Strumia A., Volansky T., 2011, *Journal of Cosmology and Astroparticle Physics*, 11, 010  
 Farrar G. R., Zaharijas G., 2006, *Physical Review Letters*, 96, 41302  
 2012PhRvL.108t1302F  
 Felizardo, M. et al. 2012, *Physical Review Letters*, 108, 201302  
 Foadi R., Frandsen M. T., Sannino F., 2009, *Physical Review D*, 80, 37702  
 Fogli G. L., Lisi E., Marrone A., Palazzo A., Rotunno A. M., 2011, *Physical Review D*, 84, 53007  
 Frandsen M., Sarkar S., 2010, *Physical Review Letters*, 105, 11301  
 Geringer-Sameth A., Koushiappas S. M., 2011, *Physical Review Letters*, 107, 241303  
 Giuliani F., 2005, *Physical Review Letters*, 95, 101301  
 Gondolo P., Edsjö J., Ullio P., Bergstrom L., Schelke M., Baltz E. A., 2004, *Journal of Cosmology and Astroparticle Physics*, 07, 008  
 Gonzalez-Garcia M. C., Maltoni M., 2008, *Physics Reports*, 460, 1  
 Gould A., 1987, *Astrophysical Journal*, 321, 571  
 Gould A., 1990, *Astrophysical Journal*, 356, 302  
 Gudnason S. B., Kouvaris C., Sannino F., 2006, *Physical Review D*, 73, 115003

- Guzik J. A., Mussack K., 2010, *The Astrophysical Journal*, 713, 1108
- Hernandez P., 2010, [arXiv:1010.4131](#)
- Hooper D., Kelso C., 2011, *Physical Review D*, 84, 83001
- Hooper D., March-Russell J., West S. M., 2005, *Physics Letters B*, 605, 228
- Imminiyaz H., Drees M., Chen X., 2011, *Journal of Cosmology and Astroparticle Physics*, 07, 003
- Jungman G., Kamionkowski M., Griest K., 1996, *Physics Reports*, 267, 195
- Kang Z., Li J., Li T., Liu T., Yang J., 2011, [arXiv:1102.5644](#)
- Kaplan D. E., Luty M. A., Zurek K. M., 2009, *Physical Review D*, 79, 115016
- Komatsu E. et al., 2011, *The Astrophysical Journal Supplement*, 192, 18
- Kurylov A., Kamionkowski M., 2004, *Physical Review D*, 69, 63503
- Lopes I., Casanellas J., Eugénio D., 2011, *Physical Review D*, 83, 63521
- Lopes I., Silk J., 2010a, *Science*, 330, 462
- Lopes I., Silk J., 2010b, *The Astrophysical Journal Letters*, 722, L95
- Lopes I. P., Silk J., 2002, *Physical Review Letters*, 88, 151303
- Lopes I. P., Silk J., Hansen S. H., 2002, *Monthly Notices of the Royal Astronomical Society*, 331, 361
- Morel P., 1997, *A & A Supplement series*, 124, 597
- Munshi D., Heavens A., Cooray A., Valageas P., 2011, *Monthly Notices of the Royal Astronomical Society*, 414, 3173
- Savage C., Gelmini G., Gondolo P., Freese K., 2009, *Journal of Cosmology and Astroparticle Physics*, 04, 010
- Scott P., Fairbairn M., Edsjö J., 2009, *Monthly Notices of the Royal Astronomical Society*, 394, 82
- Scott, P. C. Edsjö J., Fairbairn M., 2008, in *Dark Matter in Astroparticle and Particle Physics. Proceedings of the 6th International Heidelberg Conf.*, 387–392
- Serenelli A. M., Basu S., Ferguson J. W., Asplund M., 2009, *The Astrophysical Journal Letters*, 705, L123
- Serenelli A. M., Haxton W. C., Pena-Garay C., 2011, *The Astrophysical Journal*, 743, 24
- Spergel D. N., Press W. H., 1985, *Astrophysical Journal*, 294, 663
- Taoso M., Iocco F., Meynet G., Bertone G., Eggenberger P., 2010, *Physical Review D*, 82, 83509
- Turck-Chieze S., Couvidat S., 2011, *Reports on Progress in Physics*, 74, 6901
- Turck-Chieze S., Lopes I., 1993, *Astrophysical Journal*, 408, 347
- Turck-Chieze S., Palacios A., Marques J. P., Nghiem P. A. P., 2010, *The Astrophysical Journal*, 715, 1539
- Wurm M. et al., 2011, *Physical Review D*, 83, 032010